

Spectator Composes a Gravitational Canon: Spectator-field-triggered Phase Transition During Inflation and its Anisotropic Gravitational Wave Signals

Yunjia Bao^{1,*} and Keisuke Harigaya^{1,2,†}

¹*Department of Physics, Enrico Fermi Institute, Leinweber Institute for Theoretical Physics, Kavli Institute for Cosmological Physics, University of Chicago, Chicago, IL 60637, USA*

²*Kavli Institute for the Physics and Mathematics of the Universe (WPI), The University of Tokyo Institutes for Advanced Study, The University of Tokyo, Kashiwa, Chiba 277-8583, Japan*

We propose a general framework in which a phase transition is triggered during cosmic inflation by the slow-roll dynamics of a spectator field. The topological defects formed at the transition are inflated outside the horizon, reenter it after inflation, and can subsequently generate characteristic gravitational-wave (GW) signals. Quantum fluctuations of the spectator field modulate the timing of the transition, imprinting large-scale anisotropies in the resulting GW background. As an explicit realization, the spectator field may be identified with the Higgs field in a supersymmetric Standard Model. More generally, our framework applies to a wide class of spectator-modulated phenomena, providing a generic mechanism for producing anisotropic GW signals.

Introduction.—Symmetry and its spontaneous breaking are ubiquitous in particle physics. A prominent example is the electroweak symmetry, which is spontaneously broken down to the electromagnetic symmetry. In grand unified theories, gauge symmetries such as SU(5) and SO(10) are broken to the Standard Model (SM) gauge symmetry [1, 2]. In the Peccei–Quinn solution to the strong CP problem [3, 4], a global U(1) symmetry is spontaneously broken.

Symmetry breaking is often accompanied by the formation of topological defects, including magnetic monopoles, cosmic strings, and domain walls. If the symmetry breaking occurs before the observable inflation, these defects are inflated away and leave no observable imprint. Conversely, if the symmetry is broken after inflation, topological defects may give rise to observable signals, such as strong ionization by magnetic monopoles, anisotropies in the cosmic microwave background induced by cosmic strings, or gravitational waves (GWs). See Refs. [5, 6] for reviews.

Less explored, but potentially more striking, is the possibility that symmetry breaking occurs *during* the observable inflation. In this case, the resulting topological defects are inflated outside the horizon, rendering them effectively frozen by causality. After inflation ends, these defects reenter the horizon and subsequently evolve.¹ Observable consequences of this scenario include an enhanced abundance of axions [9–11] and GWs with characteristic spectral features [12–17].

In the literature, phase transitions during inflation have often been realized by coupling the symmetry

breaking sector directly to the inflaton field [14, 15, 17–25]. Such scenarios typically require a large excursion of the inflaton field value in order for the mass of the symmetry-breaking field to vary significantly during inflation.

In this Letter, we point out an alternative possibility in which a phase transition is triggered by the dynamics of a field whose energy density is subdominant during inflation, *i.e.*, a spectator field. In this setup, the timing of the phase transition is modulated by the inflationary quantum fluctuations of the spectator field. As a result, the horizon reentry of the resulting topological defects, and hence any signals they produce, is spatially modulated. In particular, if the topological defects emit GWs, this mechanism naturally generates large-scale anisotropies in the GW background.

Anisotropies in GWs sourced by scalar perturbations [26–38] and by phase transitions [39–42] have been studied previously. Compared to existing models, one of our realizations based on cosmic strings allows for the largest possible GW anisotropy while remaining consistent with constraints from (iso)curvature perturbations and their non-Gaussianity.

Light Spectator During Inflation.—Physics beyond the Standard Model typically contains new scalar fields. A notable example is supersymmetric theories, where the scalar partners of the Standard-Model fermions are predicted. If the inflationary Hubble scale H_I is larger than their masses, they may be displaced from the minimum and obtain quantum fluctuations.

We consider the case where a spectator field σ has a mass squared m_σ^2 of $\mathcal{O}(0.01 - 0.1)H_I^2$ during inflation. The mass may be a vacuum mass or a so-called Hubble-induced mass that is given by the coupling of σ with the Ricci scalar or the inflaton potential. Such a field may undergo a slow roll while obtaining de Sitter quantum fluctuations. Given an $m_\sigma^2\sigma^2/2$ potential, the equation

* yunjia.bao@uchicago.edu

† kharigaya@uchicago.edu

¹ A similar evolution of topological defects may also arise if the phase transition occurs between two stages of inflation, where the latter stage could be a period of thermal inflation [7, 8].

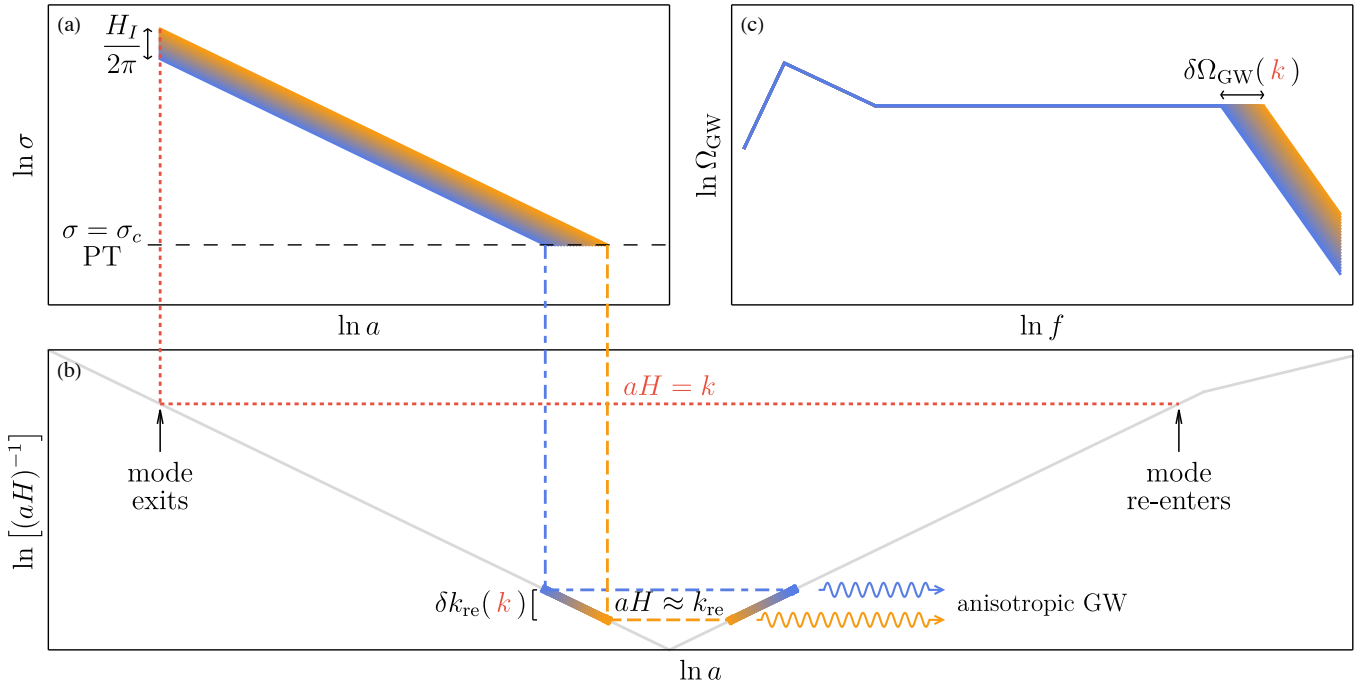


FIG. 1. Schematic of the mechanism. **Top Left (a):** A fluctuation of the spectator field value σ early in the inflation epoch imprints as a fluctuation in the phase transition (PT) timing during inflation. This changes when PT happens in different Hubble patches. **Bottom (b):** The fluctuation in PT timing at large distance k^{-1} changes the horizon size k_{re}^{-1} when the PT defects reenter. When the mode k reenters the horizon, a large-scale anisotropic gravitational-wave (GW) signal appears if the GW spectrum Ω_{GW} depends on k_{re} . **Top Right (c):** GW spectrum is modulated because of the reentry timing. Here, we take GWs produced by cosmic strings as an example. Modulation in k_{re} changes the UV rolloff scale. This modulation is at large scales because it comes from the early fluctuation of σ during inflation.

of motion for σ is

$$\ddot{\sigma} + 3H_I\dot{\sigma} \approx -m_\sigma^2\sigma \implies \sigma(t) \approx \sigma_* \exp(-\beta H_I \Delta t), \quad \beta \equiv \frac{3}{2} - \sqrt{\frac{9}{4} - \frac{m_\sigma^2}{H_I^2}}, \quad (1)$$

in which σ_* denotes the field value at some reference time t_* during inflation and Δt is the time past from t_* . Because the scale factor $a \propto e^{H_I t}$ during inflation, the classical rolling of the spectator scales as $\sigma \propto a^{-\beta}$. Taking the comoving scale that exits the horizon at each time, $k = aH_I$, as a time variable, the classical rolling of σ takes the following scale dependence,

$$\sigma(k) = \sigma_* \left(\frac{k_*}{k} \right)^\beta, \quad (2)$$

with some reference scale k_* such that $\sigma(k_*) = \sigma_*$.

On the other hand, light fields during inflation inherit fluctuations of order $\delta\sigma \sim H_I/(2\pi)$ when each mode exits the horizon [43–47]. Outside the horizon, $\delta\sigma$ and σ scales in time in the same way. Thus, the primordial dimensionless spectrum of σ is blue-tilted as

$$\Delta_\sigma^2(k) \approx \left(\frac{\delta\sigma}{\sigma(k)} \right)^2 = \left(\frac{H_I}{2\pi\sigma_*} \right)^2 \left(\frac{k}{k_*} \right)^{2\beta}. \quad (3)$$

Phase Transition During Inflation Triggered by Light Spectator.—Here, we propose the possibility that σ can trigger a phase transition during inflation. The phase transition may lead to various stochastic GW signals if it 1) produces topological defects, 2) generates large scalar fluctuations, or 3) has a strong enough phase transition strength. The precise GW spectrum depends on the dominant GW source. However, GW anisotropy is a generic feature for this class of models. We will show this with explicit examples.

We first discuss how a phase transition can be triggered by a spectator during inflation. Let us consider the following Lagrangian

$$-\mathcal{L} \supset \frac{1}{2}(\lambda_{\sigma\chi}^2\sigma^2 - m_\chi^2)\chi^2, \quad (4)$$

in which the symmetry-breaking field χ has a tachyonic mass m_χ^2 and couples quadratically to σ . Here, m_χ^2 has two potential contributions: 1) a vacuum mass $m_{\chi,0}^2$ and 2) a Hubble-induced mass $\sim c_\chi H_I^2$. For high-scale inflation, $c_\chi H_I^2 \gg m_{\chi,0}^2$ will affect the inflationary dynamics of χ . On the other hand, the vacuum expectation value (VEV) of χ today is controlled by $m_{\chi,0}^2$. We keep track of the two masses with the notation $m_{\chi,0}^2$ and $m_{\chi,I}^2 \equiv m_{\chi,0}^2 + c_\chi H_I^2$ in what follows.

Initially, when σ has a large field value, the χ field

has a positive mass and a vanishing field value. As σ slowly rolls to the origin and passes the critical value $\sigma_c = m_{\chi,I}/\lambda_{\sigma\chi}$, χ obtains a non-zero field value and undergoes a phase transition. When this phase transition happens at the comoving Hubble scale is k_{re} , then one may expect some spectral feature at this scale as it reenters the horizon after inflation.

The reentry timing of the phase transition during inflation depends on 1) the initial value of σ and 2) the number of e -foldings from the phase transition to the end of inflation. These two freedoms allow us to treat σ_* and k_* in eq. (3) as free parameters. For convenience, we may pick $k_* = k_{\text{re}}$ and $\sigma_* = \sigma_c$. From eq. (2), we find that the fluctuation in k_{re} is related to the fluctuation in σ at comoving scale k ,

$$\frac{\delta k_{\text{re}}}{k_{\text{re}}}(k) = \frac{1}{\beta} \Delta_\sigma(k) = \frac{1}{\beta} \left(\frac{H_I}{2\pi\sigma_c} \right) \left(\frac{k}{k_{\text{re}}} \right)^\beta. \quad (5)$$

Therefore, the long-wavelength fluctuation of σ imprints itself as long-wavelength modulation of k_{re} . If the GW signal from phase transition depends on k_{re} , then a large-scale anisotropic GW is expected as sketched in fig. 1. When m_χ is dominated by the Hubble-induced mass, $H_I/(2\pi\sigma_c) = \lambda_{\sigma\chi}/(2\pi c_\chi^{1/2})$, and the anisotropy is naturally large. We consider the parameter region with $\delta k_{\text{re}}/k_{\text{re}} < 1$. Otherwise, the dynamics of σ during inflation is dominated by quantum fluctuations rather than the classical rolling, and our computation is not applicable.

Gravitational-Wave Anisotropy Signal.— Large-scale fluctuations of σ may produce GW anisotropies. The multipole index ℓ of the anisotropic signal roughly scales as $\ell \approx k D_*$, in which D_* denotes the comoving distance to the emission surface of GWs. As D_* in radiation domination (RD) remains almost unchanged for earlier time, the emission surface of GWs almost coincides with the last scattering surface of the cosmic microwave background (CMB), $D_* \approx 1.4 \times 10^4$ Mpc. We will be interested in low-multipole ($\ell \lesssim 5$) anisotropies that can be observed by future GW observatories.

a. GW Anisotropy from Cosmic Strings. Consider a scalar field χ charged under some U(1) gauge symmetry that couples to the spectator field,

$$-\mathcal{L} \supset (\lambda_{\sigma\chi}^2 \sigma^2 - m_\chi^2) |\chi|^2 + \frac{\lambda_\chi^2}{4} |\chi|^4. \quad (6)$$

As σ rolls from a large value to $\sigma_c = m_{\chi,I}/\lambda_{\sigma\chi}$ during inflation, χ obtains a non-zero field value that spontaneously breaks U(1). The Kibble-Zurek mechanism can then produce cosmic strings. After inflation, these strings will have a tension of $\mu = \pi v_\chi^2$, where the VEV of χ is $v_\chi = 2m_{\chi,0}/\lambda_\chi$.

The model may be extended so that the symmetry-breaking field during inflation is different from that at the vacuum, which helps identify σ with the Higgs field in the minimal supersymmetric Standard Model (MSSM); see Appendices B and C.

The GW signature of this string network should be similar to that of a typical gauge string network, but the UV rolloff depends on the reentry Hubble scale of the inflated strings instead of the phase transition Hubble scale [55, 56]. For illustrative purposes, we simplify the GW spectrum as a broken power law²

$$\Omega_{\text{GW}} \approx 2 \times 10^{-2} \Omega_{\text{rad}} \left(\frac{g_{*,0}}{g_{*,\text{re}}} \right)^{1/3} \sqrt{\frac{\mu}{M_{\text{Pl}}^2}} \times \begin{cases} \left(\frac{f}{f_{\text{low}}} \right)^{3/2} \left(\frac{f_{\text{mid}}}{f_{\text{low}}} \right)^{1/2}, & f < f_{\text{low}}, \\ \left(\frac{f_{\text{mid}}}{f} \right)^{1/2}, & f_{\text{low}} < f < f_{\text{mid}}, \\ 1 + \left(\frac{2\pi f}{k_{\text{re}}} \right)^3, & f_{\text{mid}} < f < \frac{k_{\text{re}}}{2\pi}, \\ \left(\frac{k_{\text{re}}}{2\pi f} \right), & f > \frac{k_{\text{re}}}{2\pi}, \end{cases} \quad (7)$$

in which $\Omega_{\text{rad}} = 9.14 \times 10^{-5}$ is the current fractional density of photons and massless neutrinos, f is the frequency of the GWs, $g_{*,0(\text{re})}$ denotes the effective number of relativistic degrees of freedom today (at defects' reentry),

$$f_{\text{low}} \equiv \frac{M_{\text{Pl}}^2 H_0}{\pi v_\chi^2}, \quad f_{\text{mid}} \equiv \frac{M_{\text{Pl}}^2 k_{\text{eq}}}{\pi v_\chi^2}, \quad (8)$$

and we assume that $k_{\text{re}} \gg 2\pi f_{\text{mid}}$. The k_{re} -dependent part in the second last case corresponds to the GWs that are produced from the k_{re}^{-1} -sized loops before their decay completes. The modulation on the GW spectrum due to σ fluctuation is

$$\delta\Omega_{\text{GW}} = \frac{\delta k_{\text{re}}}{k_{\text{re}}} \frac{\partial\Omega_{\text{GW}}}{\partial \ln k_{\text{re}}}. \quad (9)$$

The GW anisotropy signal can be obtained by using eq. (5),

$$\Omega_{\text{GW, aniso}}(\ell, f) \sim 2 \times 10^{-2} \Omega_{\text{rad}} \sqrt{\frac{\mu}{M_{\text{Pl}}^2}} \left(\frac{g_{*,0}}{g_{*,\text{re}}} \right)^{1/3} \times \frac{\lambda_{\sigma\chi} H_I}{2\pi m_{\chi,I}} \frac{1}{\beta} \left(\frac{\ell}{k_{\text{re}} D_*} \right)^\beta \times \begin{cases} 3 \left(\frac{2\pi f}{k_{\text{re}}} \right)^3, & f < \frac{k_{\text{re}}}{2\pi}, \\ \frac{k_{\text{re}}}{2\pi f}, & f > \frac{k_{\text{re}}}{2\pi}. \end{cases} \quad (10)$$

Hence, one expects a slightly blue-tilted anisotropy signal, a telltale feature of the light spectator field. We offer two benchmark spectra against exclusion and reach from current and future GW observatories in fig. 2.

² Here, we focus on the GW spectrum around string reentry as it generates most of the GW anisotropy. For string loops produced later, the g_* -dependent factor should be adjusted and increase as g_* decreases.

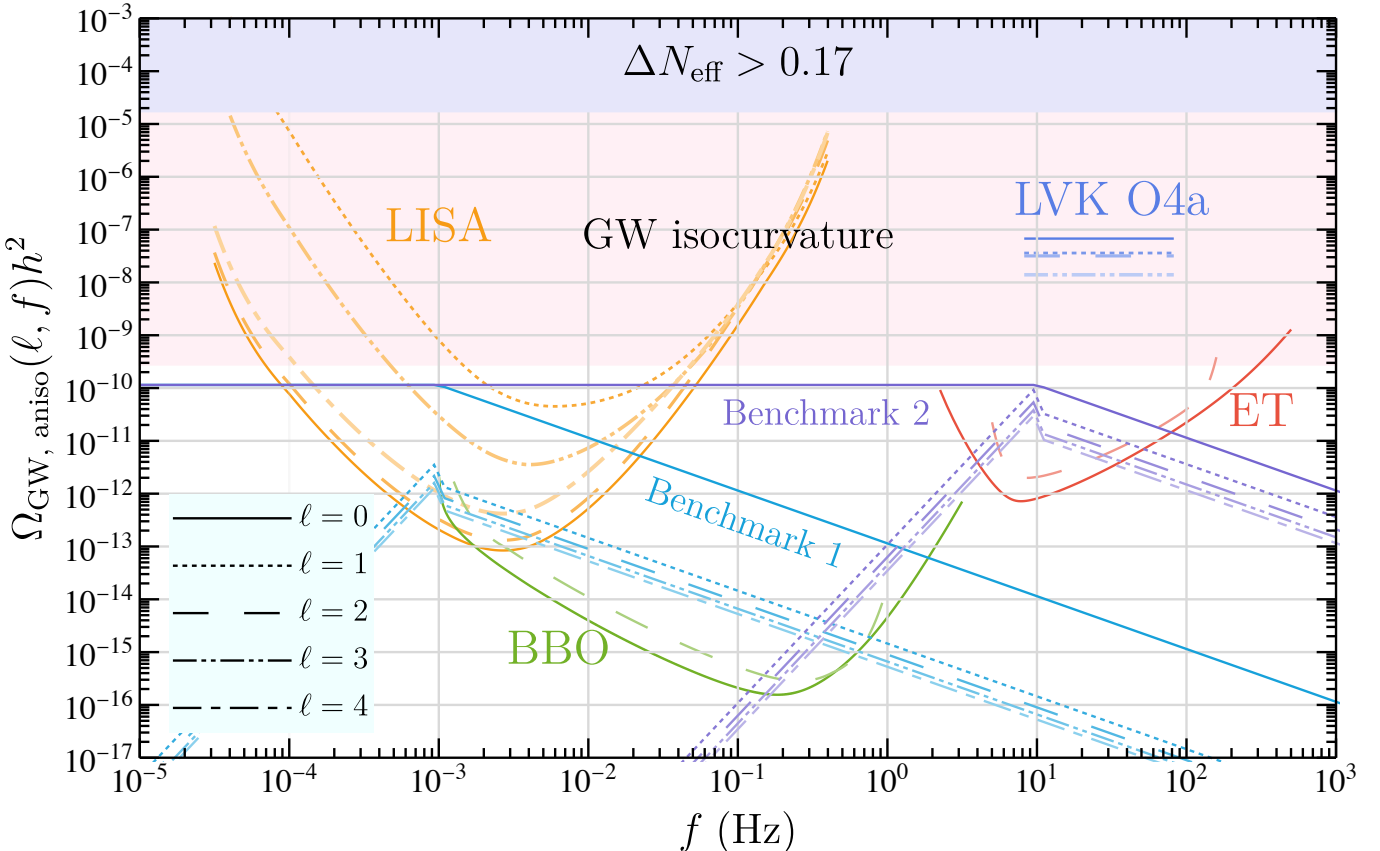


FIG. 2. Benchmark spectra for gravitational-wave (GW) anisotropy produced by spectator-modulated cosmic string reentry. While the string tension μ controls the plateau of the isotropic signal, the comoving reentry scale k_{re} of the string alters the UV rolloff scale. A modulation in k_{re} leads to an anisotropic signal $\Omega_{\text{GW, aniso}}(\ell, f)$ in higher multipoles on top of the isotropic background. Our Benchmark 1 is taken at $(\sqrt{\mu}, k_{\text{re}}/(2\pi), \beta, H_1/(2\pi\sigma_c)) = (3 \times 10^{14} \text{ GeV}, 10^{-3} \text{ Hz}, 10^{-1}, 10^{-1})$, and Benchmark 2 is taken at $(\sqrt{\mu}, k_{\text{re}}/(2\pi), \beta, H_1/(2\pi\sigma_c)) = (3 \times 10^{14} \text{ GeV}, 10 \text{ Hz}, 10^{-2}, 10^{-2})$. The current exclusions from LIGO-Virgo-KAGRA's first part of the fourth observing run (LVK O4a) [48], CMB measurement of ΔN_{eff} [49], and GW isocurvature perturbations [50] (see Appendix A 1), and the prospects of future searches (LISA [51], BBO [52, 53], and ET [52–54]) of GW anisotropy are provided for comparison. Details of the GW constraints and prospects are provided in Appendix D.

The gauge string's energy density around the string reentry is mostly radiated into GWs and can produce dark-radiation isocurvature perturbations. This computation is detailed in Appendix A 1, where we find

$$\delta\Omega_{\text{GW}}(f_{\text{peak}})h^2 \lesssim 2.8 \times 10^{-10}, \quad (11)$$

where f_{peak} is the GW frequency at which the anisotropy is maximized. For cosmic strings, $f_{\text{peak}} \simeq k_{\text{re}}/(2\pi)$. Because the isocurvature perturbations are nonlinearly related to the nearly Gaussian σ fluctuation, this leads to a local-type non-Gaussianity as well. However, our model evades the current *Planck* constraint on such non-Gaussianity [57]. See Appendix A 1 for details.

To our knowledge, this setup produces the largest GW anisotropies among the models known in the literature, without producing excessive cosmic perturbations or their non-Gaussianity. This is because almost all the energy of the source of GWs, namely, cosmic strings, goes to GWs rather than other forms of radiation [58, 59].

b. GW Anisotropy from Domain Walls. In this section, we consider another possibility that domain walls form during inflation and are pushed outside the horizon. For simplicity, we will assume that upon their reentry, the wall network immediately starts to annihilate due to bias between the false and true vacua. For concrete realization, we consider the following Lagrangian

$$-\mathcal{L} \supset \frac{1}{2}(\lambda_{\sigma\chi}^2\sigma^2 - m_\chi^2)\chi^2 + \frac{\lambda_\chi^2}{4}\chi^4 + \varepsilon^3\chi \quad (12)$$

with $\varepsilon \ll m_\chi$. The potential bias across the two vacua $\delta \sim 2m_{\chi,0}\varepsilon^3/\lambda_\chi$, while the wall tension $\tau \sim m_{\chi,0}^3/\lambda_\chi^2$. The walls immediately collapse after their horizon reentry if $\tau H_{\text{re}} < \delta$, which requires $H_{\text{re}} < \lambda_\chi\varepsilon(\varepsilon/m_{\chi,0})^2$. As H_{re} is typically small due to the inflationary dilution, it is easy to realize this inequality.

The GW spectrum can be estimated as

$$\Omega_{\text{GW}} = \Omega_{\text{rad}} \frac{0.7 \cdot \tau^2 k_{\text{eq}}^4}{24\pi M_{\text{Pl}}^4 H_{\text{eq}}^2 k_{\text{re}}^4} \times \begin{cases} \left(\frac{2\pi f}{k_{\text{re}}}\right)^3, & f \leq \frac{k_{\text{re}}}{2\pi}, \\ \left(\frac{k_{\text{re}}}{2\pi f}\right)^{n_{\text{UV}}}, & f > \frac{k_{\text{re}}}{2\pi}, \end{cases} \quad (13)$$

in which we used $H_{\text{re}} = H_{\text{eq}}(k_{\text{re}}/k_{\text{eq}})^2$ during RD. The spectral index n_{UV} is determined by detailed UV physics and is extracted numerically, and $n_{\text{UV}} \approx 1$ for scaling walls that collapse due to bias [60]. Our scenario slightly differs because the bias is already large so that the wall network collapses immediately upon reentry. Nonetheless, we expect a similar, if not sharper, UV rolloff. Then, the anisotropy signal is

$$\Omega_{\text{GW, aniso}}(\ell, f) \sim \Omega_{\text{rad}} \frac{0.7 \cdot \tau^2 k_{\text{eq}}^4}{24M_{\text{Pl}}^4 H_{\text{eq}}^2 k_{\text{re}}^4} \left(\frac{\lambda_{\sigma\chi} H_I}{2\pi m_{\chi,I}}\right) \quad (14)$$

$$\times \frac{1}{\beta} \left(\frac{\ell}{k_{\text{re}} D_*}\right)^\beta \times \begin{cases} 7 \cdot \left(\frac{2\pi f}{k_{\text{re}}}\right)^3, & f \leq \frac{k_{\text{re}}}{2\pi}, \\ (4 - n_{\text{UV}}) \left(\frac{k_{\text{re}}}{2\pi f}\right)^{n_{\text{UV}}}, & f > \frac{k_{\text{re}}}{2\pi}. \end{cases}$$

Similar to the cosmic-string case, large cosmic perturbations can be generated by the modulation of domain walls' reentry. As discussed in the Appendix A 2, we obtain a constraint

$$\delta\Omega_{\text{GW}}(f_{\text{peak}}) h^2 \lesssim \min \left\{ 2.8, 4.0 \sqrt{\frac{\Omega_{\text{GW}}}{2.3\% \Omega_{\text{rad}}}}, \right. \quad (15)$$

$$\left. 4.3 \left(\frac{\Omega_{\text{GW}}}{2.3\% \Omega_{\text{rad}}}\right)^{5/8}, 0.99 \times \left(\frac{\Omega_{\text{GW}}}{2.3\% \Omega_{\text{GW}}}\right)^{1/4} \right\} \times 10^{-10}.$$

The first constraint comes from the bound on GW isocurvature perturbations similar to the cosmic-string scenario, the second is due to the adiabatic perturbations from the radiation created by domain walls' collapse, the third is from their non-Gaussianity, and the forth is the GW isocurvature perturbations partially correlated with the curvature perturbations. This constraint is more stringent than the string case because domain walls dominantly decay into non-GW components, which obtain larger fluctuations than GWs.

Conclusion.—In this work, we have demonstrated that a phase transition modulated by a spectator field during inflation can generate sizable anisotropies in the GW background. As an explicit realization, we considered a scenario in which the timing of a phase transition during inflation is modulated by spectator-field fluctuations, leading to the formation of topological defects whose subsequent horizon reentry produces anisotropic GW signals. Although the associated (iso)curvature perturbations impose constraints on the amplitude of the anisotropy, our framework allows for $\sim \mathcal{O}(1)$ modulation of GWs on large scales. This mechanism can be naturally embedded in supersymmetric theories, where the spectator field may be identified with the Higgs field of the MSSM.

The spectator-modulated phase transition offers several advantages over scenarios in which the phase transition is modulated by the inflaton. In inflaton-modulated models, both the adiabatic perturbations and the GW anisotropies originate from inflaton fluctuations, making it difficult to generate large GW anisotropies while maintaining the observed small amplitude of adiabatic perturbations. Moreover, inflaton-modulated phase transitions typically require a large excursion of the inflaton field in order to induce a significant variation in the mass of the symmetry-breaking field during inflation. These requirements are absent in the spectator-based framework.

While our analysis focused on phase transitions triggered by the slow-roll dynamics of a spectator field, other triggering mechanisms are possible. For example, Ref. [25] studied quantum tunneling triggered by the decreasing expansion rate during inflation, where the bounce action is modulated by spectator-field fluctuations to generate curvature perturbations. If such quantum tunneling induces a phase transition, it may lead to GW signals qualitatively similar to those discussed here.

More broadly, this framework readily interfaces with a wide range of particle-physics and cosmological mechanisms. Phase transitions associated with grand unified theories, the Peccei–Quinn mechanism, or the Affleck–Dine mechanism may plausibly occur during inflation rather than before it. The framework may also be combined with other sources of GWs, such as scalar-induced tensor perturbations, to explore richer phenomenology. Finally, a spectator-modulated phase transition may itself account for the observed curvature perturbations, realizing a new class of curvaton-like models. All of these possibilities suggest that spectator-modulated phase transitions open a promising avenue for exploring the interplay between inflationary dynamics, novel cosmological observables, and fundamental particle-physics questions.

ACKNOWLEDGMENTS

We thank the enlightening comments from Soubhik Kumar. YB and KH are supported by the Department of Energy grant DE-SC0009924. KH is also supported by World Premier International Research Center Initiative (WPI), MEXT, Japan (Kavli IPMU).

Appendix A: Cosmic Perturbations from Spectator-Modulated Phase Transition

This appendix details the computation for the cosmic perturbations induced by cosmic strings and domain walls.

1. Cosmic Strings

Here, we assume that, for gauge strings, the string loops decay entirely into gravitational waves. This is sensible because the gauge and Higgs bosons of the $U(1)$ symmetry breaking have larger masses than the Hubble scale that determines the typical length scale of string reconnection and loop production.³ Because string loops redshift like matter rather than radiation, their energy density during RD can contribute significantly to the energy density of the network even when the string tension is small. In fact, the typical decay rate of string loops into GWs is $\Gamma_{\text{str}} \sim \mu H_p/M_{\text{Pl}}^2 \ll H_p$ in which H_p denotes the Hubble scale around string loop production. The typical energy density of the string loops scales as

$$\rho_{\text{loop}} \Big|_{t=\Gamma_{\text{str}}} \approx \mu H_p^2 \left(\frac{a(H_p)}{a(\Gamma_{\text{str}})} \right)^3 = \frac{\sqrt{\mu} M_{\text{Pl}}}{t^2} \approx \rho_{\text{GW}}. \quad (\text{A1})$$

Hence, during RD, a string network that reaches the scaling regime shall produce an energy density

$$\rho_{\text{long str}} \approx \mu H^2, \quad \rho_{\text{GW}} \approx \gamma \sqrt{\mu} M_{\text{Pl}} H^2, \quad (\text{A2})$$

in which $\gamma \approx 2 \times 10^{-2}$ is a dimensionless number obtained from numerical simulations [64–66]. Both the GW density produced during the scaling regime and the long-string energy density are independent of the timing of the horizon reentry of the strings, and therefore do not contribute to cosmic perturbations. On the other hand, the energy density of GWs produced by string loops right after the horizon reentry depends on the timing of the reentry and contributes to cosmic perturbations.

The curvature perturbations can be computed using the δN formalism [67–69]. To relate GW's perturbation to observational constraints, we note that the de Sitter fluctuation of σ generates uncorrelated isocurvature fluctuations in the free-streaming GW. Hence, we may recast the neutrino density isocurvature (NDI) constraint from *Planck* [50]. The NDI perturbation is defined as

$$\zeta_{\text{NDI}} \equiv 3(\zeta_{\nu} - \zeta_{\gamma}), \quad (\text{A3})$$

in which $\zeta_{\nu(\gamma)}$ are the curvature perturbations of neutrinos (photons). Here, we reinterpret ζ_{ν} as the curvature perturbations from any free-streaming species. In particular, if neutrino perturbations are generated from inflaton fluctuations, and GWs are produced from σ fluctuations, then the NDI perturbation comes from the GW

³ This argument comes from the standard Nambu-Goto approximation of cosmic strings [6] and is supported by Abelian-Higgs simulations [58, 59]. However, it is worth noting that there is debate over whether it is possible to primarily produce small string loops that can radiate massive modes [61, 62]. This leads to the small-string-loop scenario. More details about the large-string-loop and small-string-loop scenario are discussed in Ref. [63]. As our discussion focuses on semi-classical large-scale dynamics, we thus argue that gravitational wave radiation is the dominant decay channel for consistency.

from cosmic strings' reentry. To compute ζ_{ν} , we take both the initial and final slices in the scaling regime after the string reentry. The initial flat slice coincides with the uniform density slice of SM radiation. The final slice is the uniform-density slice of GWs and neutrinos. Then, the relation

$$\rho_{\text{GW},i}(\mathbf{x}) e^{-4N(\mathbf{x})} + \rho_{\nu,i} e^{-4N(\mathbf{x})} = \rho_{\text{GW}+\nu,f} \quad (\text{A4})$$

implies

$$\zeta_{\nu} = \delta N = \frac{1}{4} \frac{\delta \rho_{\text{GW}}}{\rho_{\nu} + \rho_{\text{GW}}}, \quad (\text{A5})$$

where $\delta \rho_{\text{GW}}$ is defined in the flat slice, or equivalently, in the uniform-density slice of SM radiation. Since the GW density typically has a power-law dependence $\rho_{\text{GW}} \propto k_{\text{re}}^{\alpha}$ and δk_{re} is determined by σ fluctuation as shown in eq. (2), one can relate

$$\rho_{\text{GW}} = \bar{\rho}_{\text{GW}} \left(\frac{\sigma(k)}{\bar{\sigma}(k)} \right)^{\alpha/\beta}. \quad (\text{A6})$$

Hence, to quadratic order in the Gaussian fluctuation $\delta\sigma$, the GW curvature perturbation is

$$\begin{aligned} \zeta_{\nu} &= \frac{\delta N}{\delta \rho_{\text{GW}}} \frac{\delta \rho_{\text{GW}}}{\delta \sigma} \delta \sigma + \frac{1}{2} \left[\frac{\delta^2 N}{\delta \rho_{\text{GW}}^2} \left(\frac{\delta \rho_{\text{GW}}}{\delta \sigma} \right)^2 \right. \\ &\quad \left. + \frac{\delta N}{\delta \rho_{\text{GW}}} \frac{\delta^2 \rho_{\text{GW}}}{\delta \sigma^2} \right] \delta \sigma \delta \sigma \\ &\approx \frac{1}{4} \frac{\Omega_{\text{GW}}}{\Omega_{\nu}} \frac{\alpha}{\beta} \frac{\delta \sigma}{\sigma} + \frac{1}{8} \frac{\Omega_{\text{GW}}}{\Omega_{\nu}} \left(\frac{\alpha}{\beta} \right)^2 \left(\frac{\delta \sigma}{\sigma} \right)^2, \end{aligned} \quad (\text{A7})$$

in which we used the following relations

$$\begin{aligned} \frac{\delta N}{\delta \rho_{\text{GW}}} &= \frac{1}{4(\rho_{\text{GW}} + \rho_{\nu})} \approx \frac{1}{4\rho_{\nu}}, \quad \frac{\delta^2 N}{\delta \rho_{\text{GW}}^2} \approx -\frac{1}{4\rho_{\nu}^2}, \\ \frac{\delta \rho_{\text{GW}}}{\delta \sigma} &= \frac{\alpha}{\beta} \frac{\rho_{\text{GW}}}{\sigma}, \quad \frac{\delta^2 \rho_{\text{GW}}}{\delta \sigma^2} \approx \frac{\alpha^2}{\beta^2} \frac{\rho_{\text{GW}}}{\sigma^2}, \end{aligned} \quad (\text{A8})$$

and assumed that $\rho_{\text{GW}} \ll \rho_{\nu}$ to be compatible with the ΔN_{eff} constraint from *Planck* [49] and $\beta \ll 1$ so that σ undergoes a slow roll. Therefore, the effective NDI perturbation due to GW from σ -modulated re-entry of cosmic strings is

$$\begin{aligned} \Delta_{\text{NDI}}^2 &= \left(\frac{3\Omega_{\text{GW}}}{4\Omega_{\nu}} \frac{\alpha}{\beta} \right)^2 \Delta_{\sigma}^2 \approx \left(\frac{3\Omega_{\text{rad}}}{4\Omega_{\nu}} \right)^2 \frac{\delta \Omega_{\text{GW}}^2(f_{\text{peak}})}{\Omega_{\text{rad}}^2} \\ &\approx \left(1.9 \cdot \frac{\delta \Omega_{\text{GW}}(f_{\text{peak}})}{\Omega_{\text{rad}}} \right)^2. \end{aligned} \quad (\text{A9})$$

where f_{peak} is the frequency at which the GW anisotropy is maximized. Using the *Planck* constraint at $k_{\text{low}} = 0.002 \text{ Mpc}^{-1}$ in which $\Delta_{\text{NDI}}^2(k_{\text{low}}) \lesssim 7.4\% \Delta_{\zeta}^2 \lesssim 1.6 \times 10^{-10}$, we find that

$$\delta \Omega_{\text{GW}}(f_{\text{peak}}) h^2 \lesssim 0.15 \cdot \Omega_{\text{rad}} h^2 \Delta_{\zeta}(k_{\text{low}}) \approx 2.8 \times 10^{-10}. \quad (\text{A10})$$

However, if we take the NANOGrav constraint on stable cosmic strings $G\mu \lesssim 10^{-9.5}$ [70], then we conclude that $\Omega_{\text{GW}}/\Omega_{\text{rad}} \lesssim 6.4 \times 10^{-7}$. Hence, if the NDI constraint is saturated, the GW fluctuation is at least

$$\frac{\delta\Omega_{\text{GW}}(f_{\text{peak}})}{\Omega_{\text{GW}}} \approx 0.15 \left(\frac{\Omega_{\text{rad}}}{\Omega_{\text{GW}}} \right) \Delta_\zeta \gtrsim 11, \quad (\text{A11})$$

which violates perturbativity. Therefore, requiring $\delta\Omega_{\text{GW}}(f_{\text{peak}})/\Omega_{\text{GW}} < 1$ for the cosmic-string-generated GW anisotropy and the NANOGrav constraints are typically sufficient to evade the current isocurvature constraint.

Beyond two-point correlation, it is also possible that an NDI non-Gaussianity is produced. The isocurvature fluctuation $S_{\text{NDI}}(k)$ is related to the underlying almost Gaussian field $\delta_\sigma = \delta\sigma/\sigma$ by

$$S_{\text{NDI}}(\mathbf{k}) = \frac{3}{4} \frac{\Omega_{\text{GW}}}{\Omega_\nu} \frac{\alpha}{\beta} \delta_\sigma(\mathbf{k}) + \frac{3}{8} \frac{\Omega_{\text{GW}}}{\Omega_\nu} \left(\frac{\alpha}{\beta} \right)^2 (\delta_\sigma \star \delta_\sigma)(\mathbf{k}), \quad (\text{A12})$$

in which \star denotes a momentum convolution. Then, the tree-level isocurvature bispectrum is obtained by computing $\langle S_{\text{NDI}}^3 \rangle$ of three different momenta

$$\begin{aligned} & B_{iii}(\mathbf{k}_1, \mathbf{k}_2, \mathbf{k}_3) \\ &= \frac{3^3}{4^2 \cdot 8} \left(\frac{\Omega_{\text{GW}}}{\Omega_\nu} \right)^3 \left(\frac{\alpha}{\beta} \right)^4 [2\Delta_\sigma^2(k_1)\Delta_\sigma^2(k_2) + 2 \text{ perms}]. \end{aligned} \quad (\text{A13})$$

For the cosmic string scenario, the gravitational wave spectrum is related to the NDI spectrum by eq. (A9) so that the local-type f_{NL} is

$$\begin{aligned} f_{\text{NL}}^{i,ii} &= \frac{625}{384} \left(\frac{\Omega_{\text{GW}}}{\Omega_\nu} \right)^3 \left(\frac{\delta\Omega_{\text{GW}}(f_{\text{peak}})}{\Omega_{\text{GW}} \Delta_\zeta} \right)^4 \\ &\approx 1.4 \cdot \left(\frac{\Omega_{\text{GW}}}{6.4 \times 10^{-7} \Omega_{\text{rad}}} \right)^3 \left(\frac{\delta\Omega_{\text{GW}}/\Omega_{\text{GW}}}{1} \right)^4, \end{aligned} \quad (\text{A14})$$

where we relates the curvature perturbation ζ to the gravitational potential $\Phi = 3\zeta/5$. The current constraint on the NDI non-Gaussianity from *Planck* is $|f_{\text{NL}}^{i,ii}| \lesssim 210$ [57]. As long as the NANOGrav constraint $\Omega_{\text{GW}}/\Omega_{\text{rad}} \lesssim 6.4 \times 10^{-7}$ is satisfied, the non-Gaussianity constraint is also satisfied.

It is possible that cosmic strings disappear by the nucleation or reentry of monopoles [12, 13] by the time the NANOGrav-scale GWs would be emitted. In this case, $G\mu$ may be larger and the NDI and/or non-Gaussianity may be large enough to be observed in future observations.

2. Domain Walls

For the domain wall (DW) that collapses immediately after reentry, the wall predominantly decays into other Standard Model radiation species rather than GWs.

This is because the gravitational wave emission rate is $\sim \tau/M_{\text{Pl}}^2$ in which τ denotes the wall tension while the decay rate of the network is $\sim H_{\text{re}}$ (immediate collapse upon reentry) so that $\rho_{\text{GW}} \approx \epsilon\tau\rho_{\text{DW}}/(8\pi M_{\text{Pl}}^2 H_{\text{re}})$ around walls' reentry t_{re} in which the efficiency factor $\epsilon \approx 0.7$ [60] and $\rho_{\text{DW}}(t_{\text{re}}) = \tau H_{\text{re}}$. If DWs' reentry happens during RD, we can express

$$\begin{aligned} \frac{\rho_{\text{GW}}}{\rho_{\text{rad}}} &= \frac{3\epsilon}{8\pi} \left(\frac{\rho_{\text{DW}}}{\rho_{\text{rad}}} \right)^2 \\ \implies \frac{\rho_{\text{DW}}}{\rho_{\text{rad}}} &= \left(\frac{g_{*,\text{re}}}{g_{*,0}} \right)^{1/6} \sqrt{\frac{8\pi}{3\epsilon} \frac{\Omega_{\text{GW}}}{\Omega_{\text{rad}}}}, \end{aligned} \quad (\text{A15})$$

where $\rho_{\text{DW}}/\rho_{\text{rad}}$ is evaluated around the reentry while $\Omega_{\text{GW}}/\Omega_{\text{rad}}$ is evaluated today.

On the other hand, the SM radiation from domain walls observed at a later time t_f will obtain an energy density $\rho_{\text{DW}}(t_f) = \tau H_{\text{re}}(T_f/T_{\text{re}})^4 \propto T_{\text{re}}^{-2}$. Thus, we can track the curvature perturbation by treating the original SM radiation and that generated by DW decay separately as a radiation fluid with density ρ_{SM} and another with ρ_{DW} . Assuming $\rho_{\text{DW}} \ll \rho_{\text{SM}} \approx \rho_{\text{rad}}$ (which is required to avoid domain-wall-dominated epoch), we may take the initial flat slice at some temperature $T_* < T_{\text{re}}$ of the SM radiation and take the final slice at a uniform-density slice of SM + DW fluid and enforce

$$T_*^4 e^{-4N(\mathbf{x})} + \frac{\tau}{M_{\text{Pl}}} T_{\text{re}}^2(\mathbf{x}) \left(\frac{T_*}{T_{\text{re}}(\mathbf{x})} \right)^4 e^{-4N(\mathbf{x})} = \rho_{\text{rad}}, \quad (\text{A16})$$

which implies that the curvature perturbation from DW-generated radiation is

$$\zeta_{\text{DW}} = -\frac{1}{2} \frac{\rho_{\text{DW}}}{\rho_{\text{rad}}} \frac{\delta T_{\text{re}}}{T_{\text{re}}} = \frac{1}{4} \frac{\delta \rho_{\text{DW}}}{\rho_{\text{rad}}}, \quad (\text{A17})$$

in which we used the relation that $\delta T_{\text{re}}/T_{\text{re}} = -\delta \rho_{\text{DW}}/(2\rho_{\text{DW}})$. And a subdominant curvature perturbation due to GW is

$$\begin{aligned} \frac{\delta \rho_{\text{GW}}}{\rho_{\text{GW}}} &= 2 \frac{\rho_{\text{rad}}}{\rho_{\text{DW}}} \frac{\delta \rho_{\text{DW}}}{\rho_{\text{rad}}} = 8 \frac{\rho_{\text{rad}}}{\rho_{\text{DW}}} \zeta_{\text{DW}} \\ &= \left(\frac{g_{*,0}}{g_{*,\text{re}}} \right)^{1/6} \sqrt{\frac{24\epsilon}{\pi} \frac{\Omega_{\text{rad}}}{\Omega_{\text{GW}}}} \zeta_{\text{DW}}, \end{aligned} \quad (\text{A18})$$

in which we used eq. (A15). Thus, the adiabatic constraint on ζ_{DW} limits the anisotropic GW signal to be below

$$\begin{aligned} \delta\Omega_{\text{GW}}(f_{\text{peak}})h^2 &\lesssim \left(\frac{g_{*,0}}{g_{*,\text{re}}} \right)^{1/6} \sqrt{\frac{24\epsilon}{\pi} \frac{\Omega_{\text{GW}}}{\Omega_{\text{rad}}}} \Omega_{\text{rad}} h^2 \Delta_\zeta(k_{\text{low}}) \\ &\approx 4.0 \times 10^{-10} \sqrt{\frac{\Omega_{\text{GW}}}{2.3\% \Omega_{\text{rad}}}} \left(\frac{106.75}{g_{*,\text{re}}} \right)^{1/6}. \end{aligned} \quad (\text{A19})$$

When the ΔN_{eff} constraint is saturated by taking $\Omega_{\text{GW}} = 2.3\% \Omega_{\text{rad}}$, this is a weaker constraint than the NDI constraint $\delta\Omega_{\text{GW}}(f_{\text{peak}})h^2 \lesssim 2.8 \times 10^{-10}$. However, for generically lower isotropic background Ω_{GW} , this is a

stronger constraint. Alternatively, one may compare the constraint on the GW fluctuation, *i.e.*,

$$\frac{\delta\Omega_{\text{GW}}(f_{\text{peak}})}{\Omega_{\text{GW}}} \lesssim 4.2 \times 10^{-4} \sqrt{\frac{2.3\%\Omega_{\text{rad}}}{\Omega_{\text{GW}}}} \left(\frac{106.75}{g_{*,\text{re}}} \right)^{1/6}. \quad (\text{A20})$$

The adiabatic-perturbation constraint remains strong until $\Omega_{\text{GW}}h^2 \lesssim 1.7 \times 10^{-13}$ at which the perturbativity constraint $\delta\Omega_{\text{GW}} < \Omega_{\text{GW}}$ becomes effective.

Non-Gaussianity of the DW-originated fluctuations can be obtained by expanding to 2nd-order in $\delta\sigma$,

$$\zeta_{\text{DW}} \approx \frac{1}{2\beta} \frac{\rho_{\text{DW}}}{\rho_{\text{rad}}} \frac{\delta\sigma}{\sigma} + \frac{1}{2\beta^2} \frac{\rho_{\text{DW}}}{\rho_{\text{rad}}} \frac{\delta\sigma^2}{\sigma^2}, \quad (\text{A21})$$

leading to a local f_{NL} of the form

$$\begin{aligned} f_{\text{NL}}^{a,aa} &\approx \frac{5}{3} \frac{1}{2^3 \beta^4} \left(\frac{\rho_{\text{DW}}}{\rho_{\text{rad}}} \right)^3 \left(\frac{\beta}{4} \right)^4 \left(\frac{\delta\Omega_{\text{GW}}(f_{\text{peak}})}{\Omega_{\text{GW}} \Delta_{\zeta}} \right)^4 \\ &= \frac{5}{12} \sqrt{\frac{g_{*,\text{re}}}{g_{*,0}}} \left(\frac{\pi}{24\epsilon} \frac{\Omega_{\text{GW}}}{\Omega_{\text{rad}}} \right)^{3/2} \left(\frac{\delta\Omega_{\text{GW}}(f_{\text{peak}})}{\Omega_{\text{GW}} \Delta_{\zeta}} \right)^4 \end{aligned} \quad (\text{A22})$$

assuming $\Delta_{\text{DW}}^2 \ll \Delta_{\zeta}^2$ which holds when $(\rho_{\text{DW}}/\rho_{\text{rad}})(\dot{\phi}/\dot{\sigma}) \ll 1$. Recasting the *Planck* constraint $|f_{\text{NL}}^{a,aa}| \lesssim 5.1$ [57], we find that the anisotropic GW signal must be smaller than

$$\delta\Omega_{\text{GW}}(f_{\text{peak}})h^2 \lesssim 4.3 \times 10^{-10} \left(\frac{\Omega_{\text{GW}}}{2.3\%\Omega_{\text{rad}}} \right)^{5/8} \left(\frac{106.75}{g_{*,\text{re}}} \right)^{1/8}. \quad (\text{A23})$$

Lastly, this type of signal also induces correlated isocurvature. The correlation is

$$\begin{aligned} \langle S_{\nu} \zeta_{\text{DW}} \rangle &= \frac{3}{4} \left(\frac{g_{*,\text{re}}}{g_{*,0}} \right)^{1/6} \sqrt{\frac{\pi}{24\epsilon}} \frac{\Omega_{\text{rad}}}{\Omega_{\nu}} \\ &\times \left(\frac{\Omega_{\text{GW}}}{\Omega_{\text{rad}}} \right)^{3/2} \left(\frac{\delta\Omega_{\text{GW}}(f_{\text{peak}})}{\Omega_{\text{GW}}} \right)^2. \end{aligned} \quad (\text{A24})$$

The *Planck* constraint $\langle S_{\nu} \zeta_{\text{DW}} \rangle < 5 \times 10^{-11}$ [50] requires

$$\delta\Omega_{\text{GW}}h^2 \lesssim 9.9 \times 10^{-11} \left(\frac{\Omega_{\text{GW}}}{2.3\%\Omega_{\text{rad}}} \right)^{1/4} \left(\frac{106.75}{g_{*,\text{re}}} \right)^{1/12}. \quad (\text{A25})$$

Although the correlated isocurvature constraint is the strongest one for the benchmark of Ω_{GW} here, because the $f_{\text{NL}}^{a,aa}$ constraint $\propto \Omega_{\text{GW}}^{5/8}$ drops quicker than $\Omega_{\text{GW}}^{1/4}$ as Ω_{GW} decreases, the $f_{\text{NL}}^{a,aa}$ constraint eventually becomes stronger at small Ω_{GW} .

Appendix B: Symmetry Breaking by Two Fields

In the main text, we consider a case where a charged field breaks symmetry during inflation and remains the

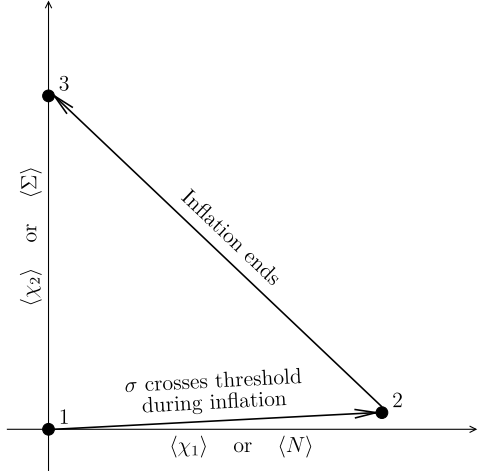


FIG. 3. Schematic for the evolution of the field values in the two-field symmetry breaking discussed in App. B. Initially, both charge-1 field χ_1 and charge-2 field χ_2 have no field values during inflation. When the spectator field σ crosses a threshold, χ_1 rolls to a minimum generated by the tachyonic Hubble-induced mass. χ_2 field may obtain a tiny field value by coupling to χ_1 . After inflation, χ_1 's Hubble-induced mass term becomes negligible while χ_2 's tachyonic vacuum mass becomes significant and drives χ_2 to a new field value. In the supersymmetric realization, χ_1 can be identified with right-handed sneutrino N , χ_2 with the $B - L$ breaking scalar, and σ with the Higgs field as discussed in App. C.

dominant source of symmetry breaking also in the vacuum. This setup may be slightly varied so that the symmetry-breaking field during inflation is different from that in the vacuum.

For example, let us introduce two fields χ_1 and χ_2 , where the subscript shows the U(1) charge of each field, and consider the Lagrangian of the form

$$\begin{aligned} -\mathcal{L} &= (\lambda_{\sigma\chi}^2 \sigma^2 - c_1 H_I^2 + m_1^2) |\chi_1|^2 + \frac{\lambda_1^2}{4} |\chi_1|^4 \\ &+ (c_2 H_I^2 - m_2^2) |\chi_2|^2 + \frac{\lambda_2^2}{4} |\chi_2|^4 + (\Lambda \chi_1^2 \chi_2^* + \text{h.c.}). \end{aligned} \quad (\text{B1})$$

During inflation, assuming $c_1 H_I^2 > m_1^2$, χ_1 breaks the U(1) symmetry and produces cosmic strings. Assuming $c_2 H_I^2 > m_2^2$, χ_2 is trapped near the origin, but because of the interaction term between χ_1 and χ_2 , χ_2 obtains a non-zero field value. Parameterizing the fields as $\chi_i \sim v_i e^{i\theta_i}$, the interaction term $\propto \cos(\theta_2 - 2\theta_1)$, so χ_2 winds twice more around the cosmic strings than χ_1 , which χ_1 typically winds once around strings. Then, as the Hubble-induced mass of χ_1 becomes small after inflation, the VEV of χ_1 vanishes while U(1) continues to be broken by χ_2 , with cosmic strings made by χ_2 . The evolution of the field values is sketched in fig. 3.

Appendix C: Model Realization: GW Anisotropy from Higgs-driven $B - L$ Strings

So far, we have discussed our mechanism within a toy model. We now embed the mechanism into a well-motivated UV extension of the SM. To this end, we consider supersymmetric theory, in which the lightness of σ and χ can be understood in terms of supersymmetry.

To be concrete, we consider $U(1)_{B-L}$ phase transition and shows that the Higgs fields in the minimal supersymmetric SM (MSSM) can play the role of σ . Besides the MSSM fields, we introduce a right-handed neutrino field N with $B-L$ charge 1, a scalar Σ with $B-L$ charge -2 , and another $\bar{\Sigma}$ field with $B-L$ charge 2 to ensure anomaly cancellation. We start by considering the following superpotential

$$W = yLH_uN + \frac{\lambda}{2}\Sigma N^2. \quad (C1)$$

This leads to the following Lagrangian

$$\begin{aligned} -\mathcal{L} \supset & \left(|y|^2 |H_u|^2 - c_N H_I^2 + m_{\text{soft}}^2 \right) |N|^2 \\ & + \left(|\lambda|^2 |N|^2 + c_\Sigma H_I^2 - m_{\text{soft}}^2 \right) |\Sigma|^2 \\ & + (c_{\bar{\Sigma}} H_I^2 - m_{\text{soft}}^2) |\bar{\Sigma}|^2 \\ & + (\lambda m_{\text{soft}} \Sigma N^2 + \text{h.c.}) \\ & + \frac{|\lambda|^2}{4} |N|^4 + \frac{g_{B-L}^2}{2} \left(|N|^2 - 2|\Sigma|^2 + 2|\bar{\Sigma}|^2 \right)^2, \end{aligned} \quad (C2)$$

where we took $L = 0$, which can be guaranteed by a large enough positive mass of L . We omit the D -term potential by the MSSM gauge group, and in the following, H_u is understood as a D -flat direction $H_u H_d$ that plays the role of the light spectator. Heavy neutral slepton N is the field χ_1 undergoing phase transition during inflation, and Σ is the field χ_2 that breaks $U(1)_{B-L}$ at the vacuum.

Initially, H_u has a large field value but is light during inflation, while other fields have vanishing field values. As it scans to the critical value $H_u \lesssim \sqrt{c_N} H_I / y$, N undergoes a phase transition, producing $B-L$ gauge strings. We may assume that $\lambda < g_{B-L}$ such that the D -term potential of N field dominates and fixes N to obtain a field value $\langle N \rangle \simeq \sqrt{c_N} H_I / g_{B-L}$. By setting $g_{B-L} < 1$ or $c_N > 1$, N can be fixed to a field value larger than H_I with a larger mass so that its de Sitter fluctuation can be suppressed, and N 's phase transition is complete during inflation. In the meantime, the Σ field is also nudged away from zero because of the A -term potential. The new field value of Σ is $\langle \Sigma \rangle \simeq c_N \lambda m_{\text{soft}} / (c_\Sigma g_{B-L}^2)$ with a winding dictated by the winding of N field. Hence, Σ strings are formed during inflation as well. $\bar{\Sigma}$ does not need to obtain a field value yet, which can be accommodated by a positive Hubble-induced mass.

After inflation, $\langle N \rangle$ decreases due to the positive vacuum mass. $\langle \Sigma \rangle$ and $\langle \bar{\Sigma} \rangle$ increase because of negative soft mass terms. D -flatness ensures that $\langle \Sigma \rangle \sim \langle \bar{\Sigma} \rangle$. To

stabilize the $\langle \Sigma \rangle$ and $\langle \bar{\Sigma} \rangle$, we have two options: 1) introducing another singlet X or 2) considering a radiative breaking of $U(1)_{B-L}$.

The following superpotential realizes the first case

$$W \supset \kappa X (\Sigma \bar{\Sigma} - v^2) \quad (C3)$$

so that the F term of X forms a wine-bottle potential $\sim \kappa^2 |\Sigma \bar{\Sigma} - v^2|^2$. If $\kappa \lesssim \sqrt{c_\Sigma + c_{\bar{\Sigma}}} H_I / v$, the tachyonic mass term is negligible during inflation and will not affect the symmetry-breaking pattern discussed in the previous paragraphs. Once $\langle \Sigma \rangle \sim \langle \bar{\Sigma} \rangle \sim v$, N strings formed during inflation will be wrapped around by Σ and $\bar{\Sigma}$ field, and the D -term potential can ensure a safe transfer of the winding. Although the A -term potential winds the Σ field twice around the N field, the non-minimal Σ strings remain stable until reentry because $g_{B-L} > \kappa$ leads to an attractive force binding two minimal Σ strings together. Also, the post-inflationary breaking of $\bar{\Sigma}$ can produce another cosmic string due to the breaking of the global chiral symmetry of Σ and $\bar{\Sigma}$. This string, however, is not stable because the $\kappa^2 v^2 \Sigma \bar{\Sigma}$ term explicitly breaks the chiral symmetry.

More minimally, one may assume that the soft mass of Σ gets radiatively corrected to obtain a minimum [71]

$$-\mathcal{L} \simeq m_{\text{soft}}^2 \left[1 + \left(\frac{\lambda}{4\pi} \right)^2 \ln \left(\frac{\Sigma^2}{\Lambda^2} \right) \right] \Sigma^2, \quad (C4)$$

which yields $\langle \Sigma \rangle \simeq \Lambda \exp(-4\pi/\lambda)^2$. In this case, the breaking of $\bar{\Sigma}$ string produces a stable global string besides the $U(1)_{B-L}$ string, and the Nambu-Goldstone boson of this global symmetry can be massless without further explicit breaking. However, as long as $v \lesssim 10^{-2} M_{\text{Pl}}$, the Nambu-Goldstone radiation from global strings can evade the ΔN_{eff} constraint as the string network in the scaling regime is a subdominant component of the radiation bath.

We considered the case where $H_u H_d$ is σ and N is χ , but other combinations are possible. For example, with $H_u H_d$ being σ , $LL\bar{e}$ may be χ . Also, X may play the role of σ with $\Sigma \bar{\Sigma}$ being χ .

Appendix D: Sensitivities for GW Anisotropy

In this appendix, we detail how sensitivities of current and future GW observatories are recasted in this paper. We match our $\Omega_{\text{GW, aniso}}^m(\ell, f)$ to the spherical harmonic coefficients $\Omega_{\text{GW}, \ell}^m$ of the directional GW spectrum

$$\Omega_{\text{GW}}(\hat{n}, f) = \sum_{\ell, m} \Omega_{\text{GW}, \ell}^m Y_\ell^m(\hat{n}) \quad (D1)$$

on the celestial sphere [51, 52]. Because $Y_0^0(\hat{n}) = 1/\sqrt{4\pi}$, the monopole coefficient is larger than the usual isotropic spectrum $\Omega_{\text{GW}, \ell=0}^{m=0} = \sqrt{4\pi} \Omega_{\text{GW}}$. In other words, the sky-averaged spectrum $\Omega_{\text{GW}}(f) = (4\pi)^{-1} \int d^2 \hat{n} \Omega_{\text{GW}}(\hat{n}, f)$

is dimensionless while $\Omega_{\text{GW},\ell}^m$ has a unit $\text{sr}^{1/2}$ as $Y_\ell^m(\hat{n})$ has a unit $\text{sr}^{-1/2}$. Another frequently used convention is to define $\Omega_{\text{GW}}(f) = \int d^2\hat{n} \tilde{\Omega}_{\text{GW}}(\hat{n}, f)$ and perform an expansion using dimensionless spherical harmonic function $\tilde{Y}_\ell^m(\hat{n}) = \sqrt{4\pi} Y_\ell^m(\hat{n})$. In this expansion convention, the spherical harmonic coefficient $\tilde{\Omega}_{\text{GW},\ell}^m$ has a unit sr^{-1} .

Sometimes, one also introduces the relative directional fluctuation

$$\delta_{\text{GW}}(\hat{n}, f) = \frac{\Omega_{\text{GW}}(\hat{n}, f) - \Omega_{\text{GW}}(f)}{\Omega_{\text{GW}}(f)}, \quad (\text{D2})$$

$$\delta_{\text{GW},\ell}^m = \int d^2\hat{n} Y_\ell^{m*}(\hat{n}) \delta_{\text{GW}}(\hat{n}, f) \quad (\text{D3})$$

in which $\delta_{\text{GW},\ell}^m$ has a unit $\text{sr}^{1/2}$ and define the variance of its spherical harmonic coefficient as

$$\langle \delta_{\text{GW},\ell}^{m*} \delta_{\text{GW},\ell'}^{m'} \rangle = \delta_{\ell'\ell} \delta_{m'm} C_\ell \quad (\text{D4})$$

analogous to the CMB measurement so that

$$\Omega_{\text{GW},\ell}^m \approx \sqrt{C_\ell} \Omega_{\text{GW}}(f) \quad (\text{D5})$$

from a steradian counting. For the other convention widely used in GW observatories [48, 72], one sometimes define a different \tilde{C}_ℓ

$$\langle \tilde{\Omega}_{\text{GW},\ell}^{m*} \tilde{\Omega}_{\text{GW},\ell'}^{m'} \rangle = \delta_{\ell'\ell} \delta_{m'm} \tilde{C}_\ell, \quad (\text{D6})$$

in which \tilde{C}_ℓ has a dimension sr^{-2} . Then, the spherical harmonic coefficients relates to this \tilde{C}_ℓ via

$$\Omega_{\text{GW},\ell}^m \approx (4\pi)^{3/2} \sqrt{\tilde{C}_\ell} \quad (\text{D7})$$

Lastly, much similar to the CMB C_ℓ , the per-log- ℓ power spectrum is given by $\sqrt{\ell(\ell+1)C_\ell/(2\pi)}$ [38, 56]; therefore, when we plot the benchmark $\Omega_{\text{GW, aniso}}(\ell, f)$ spectrum from modulated reentry of cosmic strings, we introduce another factor of $\sqrt{2\pi}[\ell(\ell+1)]^{-1/2}$ to convert the estimated per-log- ℓ $\Omega_{\text{GW, aniso}}(\ell, f)$ to $\Omega_{\text{GW},\ell}^m(f)$.

For sensitivity curves of GW observatories, it is common to project the reach using the power-law-integrated sensitivity (PLIS) curve Ω_{PLIS} [53, 73, 74]. This reach is typically much deeper than per-frequency-bin (strain-noise) sensitivity as one usually integrate over multiple frequency bins to search a particular primordial signal. This is usually determined by the number of detectors n_{det} , observation time t_{obs} , effective noise spectrum Ω_N , and a signal-to-noise-ratio threshold ϱ_{thr} . The PLIS is defined as

$$\begin{aligned} \Omega_{\text{PLIS}}(f) \\ \equiv \max_p \left\{ \varrho_{\text{thr}} \left[n_{\text{det}} t_{\text{obs}} \int_{f_{\text{min}}}^{f_{\text{max}}} df \left(\frac{(f/f_{\text{ref}})^p}{\Omega_N(f)} \right)^2 \right]^{-1/2} \right. \\ \left. \times \left(\frac{f}{f_{\text{ref}}} \right)^p \right\}. \end{aligned} \quad (\text{D8})$$

Here, we pick $t_{\text{obs}} = 1 \text{ yr}$ and $\varrho_{\text{thr}} = 1$ to project reaches for future detectors, such as LISA, Einstein Telescope (ET), Big Bang Observer (BBO), and use the noise spectra from Refs. [51, 52] for anisotropic reach and Ref. [53] for the isotropic reach. In addition, the first part of the fourth observing run of the LIGO-Virgo-KAGRA network (LVK O4a) also limits on the GW anisotropy on a scale-invariant spectrum [48]. While different from PLIS, this still provides valuable insights on current exclusions. We cast these constraints on \tilde{C}_ℓ to $\Omega_{\text{GW},\ell}^m$ and place them at the frequency ranges where the LVK detectors is the most sensitive. Lastly, we also used an ET sensitivity projection for the scale-invariant spectrum from Ref. [54] as a consistency check with other projections.

[1] H. Georgi and S. L. Glashow, Unity of All Elementary Particle Forces, *Phys. Rev. Lett.* **32**, 438 (1974).

[2] H. Fritzsch and P. Minkowski, Unified Interactions of Leptons and Hadrons, *Ann. Phys.* **93**, 193 (1975).

[3] R. D. Peccei and H. R. Quinn, CP Conservation in the Presence of Instantons, *Phys. Rev. Lett.* **38**, 1440 (1977).

[4] R. D. Peccei and H. R. Quinn, Constraints Imposed by CP Conservation in the Presence of Instantons, *Phys. Rev. D* **16**, 1791 (1977).

[5] A. Vilenkin, Cosmic Strings and Domain Walls, *Phys. Rept.* **121**, 263 (1985).

[6] A. Vilenkin and E. P. S. Shellard, *Cosmic Strings and Other Topological Defects*, reprint ed., Cambridge monographs on mathematical physics (Cambridge University Press, Cambridge [u.a.]: Cambridge Univ. Press, 2000).

[7] K. Yamamoto, Phase Transition Associated With Intermediate Gauge Symmetry Breaking in Superstring Models, *Phys. Lett. B* **168**, 341 (1986).

[8] D. H. Lyth and E. D. Stewart, Thermal inflation and the moduli problem, *Phys. Rev. D* **53**, 1784 (1996), arXiv:hep-ph/9510204.

[9] P. Baratella, A. Pomarol, and F. Rompineve, The Supercooled Universe, *JHEP* **03** (3), 100, arXiv:1812.06996 [hep-ph].

[10] M. Redi and A. Tesi, Meso-inflationary QCD axion, *Phys. Rev. D* **107**, 095032 (2023), arXiv:2211.06421 [hep-ph].

[11] K. Harigaya and L.-T. Wang, More axions from diluted domain walls, arXiv 10.48550/arxiv.2211.08289 (2022), arXiv:2211.08289 [hep-ph].

[12] X. Martin and A. Vilenkin, Gravitational wave background from hybrid topological defects, *Phys. Rev. Lett.* **77**, 2879 (1996), arXiv:astro-ph/9606022.

[13] X. Martin and A. Vilenkin, Gravitational radiation from monopoles connected by strings, *Phys. Rev. D* **55**, 6054 (1997), arXiv:gr-qc/9612008.

[14] G. Lazarides, R. Maji, and Q. Shafi, Cosmic strings, inflation, and gravity waves, *Phys. Rev. D* **104**, 095004 (2021), arXiv:2104.02016 [hep-ph].

[15] R. Maji and Q. Shafi, Monopoles, strings and gravitational waves in non-minimal inflation, *JCAP* **03** (03), 007, arXiv:2208.08137 [hep-ph].

[16] Y. Bao, K. Harigaya, and L.-T. Wang, Crescendo beyond the horizon: more gravitational waves from domain walls bounded by inflated cosmic strings, *JHEP* **11** (11), 032, arXiv:2407.17525 [hep-ph].

[17] R. Maji, A. Moursy, and Q. Shafi, Induced gravitational waves, metastable cosmic strings and primordial black holes in GUTs, *JCAP* **01** (01), 106, arXiv:2409.13584 [hep-ph].

[18] V. N. Senoguz and Q. Shafi, Primordial monopoles, proton decay, gravity waves and GUT inflation, *Phys. Lett. B* **752**, 169 (2016), arXiv:1510.04442 [hep-ph].

[19] H. An, K.-F. Lyu, L.-T. Wang, and S. Zhou, A unique gravitational wave signal from phase transition during inflation*, *Chin. Phys. C* **46**, 101001 (2020), arXiv:2009.12381 [astro-ph.CO].

[20] J. Chakrabortty, G. Lazarides, R. Maji, and Q. Shafi, Primordial Monopoles and Strings, Inflation, and Gravity Waves, *JHEP* **02** (2), 114, arXiv:2011.01838 [hep-ph].

[21] H. An, K.-F. Lyu, L.-T. Wang, and S. Zhou, Gravitational waves from an inflation triggered first-order phase transition, *JHEP* **06** (6), 050, arXiv:2201.05171 [astro-ph.CO].

[22] H. An and C. Yang, Gravitational waves produced by domain walls during inflation, *Phys. Rev. D* **109**, 123508 (2024), arXiv:2304.02361 [hep-ph].

[23] H. An, B. Su, H. Tai, L.-T. Wang, and C. Yang, Phase transition during inflation and the gravitational wave signal at pulsar timing arrays, *Phys. Rev. D* **109**, L121304 (2024), arXiv:2308.00070 [astro-ph.CO].

[24] H. An, Q. Chen, Y. Li, and Y. Yin, Large non-Gaussianities corresponding to first-order phase transitions during inflation, arXiv 10.48550/arxiv.2411.12699 (2024), arXiv:2411.12699 [hep-ph].

[25] B. Garbrecht, P. S. Ghoderao, and A. Rajantie, Curvature perturbations from vacuum transition during inflation, *JCAP* **05** (05), 049, arXiv:2502.01632 [astro-ph.CO].

[26] N. Bartolo, D. Bertacca, S. Matarrese, M. Peloso, A. Ricciardone, A. Riotto, and G. Tasinato, Anisotropies and non-Gaussianity of the Cosmological Gravitational Wave Background, *Phys. Rev. D* **100**, 121501 (2019), arXiv:1908.00527 [astro-ph.CO].

[27] N. Bartolo, D. Bertacca, S. Matarrese, M. Peloso, A. Ricciardone, A. Riotto, and G. Tasinato, Characterizing the cosmological gravitational wave background: Anisotropies and non-Gaussianity, *Phys. Rev. D* **102**, 023527 (2020), arXiv:1912.09433 [astro-ph.CO].

[28] E. Dimastrogiovanni, M. Fasiello, A. Malhotra, and G. Tasinato, Enhancing gravitational wave anisotropies with peaked scalar sources, *JCAP* **01** (01), 018, arXiv:2205.05644 [astro-ph.CO].

[29] C. Chen and A. Ota, Induced gravitational waves from statistically anisotropic scalar perturbations, *Phys. Rev. D* **106**, 063507 (2022), arXiv:2205.07810 [astro-ph.CO].

[30] J.-P. Li, S. Wang, Z.-C. Zhao, and K. Kohri, Primordial non-Gaussianity f_{NL} and anisotropies in scalar-induced gravitational waves, *JCAP* **10** (10), 056, arXiv:2305.19950 [astro-ph.CO].

[31] J.-P. Li, S. Wang, Z.-C. Zhao, and K. Kohri, Complete analysis of the background and anisotropies of scalar-induced gravitational waves: primordial non-Gaussianity f_{NL} and g_{NL} considered, *JCAP* **06** (06), 039, arXiv:2309.07792 [astro-ph.CO].

[32] S. Wang, Z.-C. Zhao, J.-P. Li, and Q.-H. Zhu, Implications of pulsar timing array data for scalar-induced gravitational waves and primordial black holes: Primordial non-Gaussianity f_{NL} considered, *Phys. Rev. Res.* **6**, L012060 (2024), arXiv:2307.00572 [astro-ph.CO].

[33] Y.-H. Yu and S. Wang, Anisotropies in scalar-induced gravitational-wave background from inflaton-curvaton mixed scenario with sound speed resonance, *Phys. Rev. D* **109**, 083501 (2024), arXiv:2310.14606 [astro-ph.CO].

[34] J. Á. Ruiz and J. Rey, Gravitational waves in ultra-slow-roll and their anisotropy at two loops, *JCAP* **04** (04), 026, arXiv:2410.09014 [astro-ph.CO].

[35] J. Rey, A consistency relation for induced gravitational wave anisotropies, arXiv 10.48550/arxiv.2411.08873 (2024), arXiv:2411.08873 [astro-ph.CO].

[36] J.-P. Li, S. Wang, Z.-C. Zhao, and K. Kohri, The isotropy, anisotropies and non-Gaussianity of the scalar-induced gravitational-wave background: diagram-

matic approach for primordial non-Gaussianity up to any order, arXiv 10.48550/arxiv.2505.16820 (2025), arXiv:2505.16820 [astro-ph.CO].

[37] Y.-H. Yu and S. Wang, Large anisotropies in the gravitational wave background from baryogenesis, arXiv 10.48550/arxiv.2504.07838 (2025), arXiv:2504.07838 [astro-ph.CO].

[38] A. Bodas, K. Harigaya, K. Inomata, T. Terada, and L.-T. Wang, Anisotropic Gravitational Waves from Anisotropic Axion Rotation, arXiv 10.48550/arxiv.2508.08249 (2025), arXiv:2508.08249 [hep-ph].

[39] M. Geller, A. Hook, R. Sundrum, and Y. Tsai, Primordial Anisotropies in the Gravitational Wave Background from Cosmological Phase Transitions, *Phys. Rev. Lett.* **121**, 201303 (2018), arXiv:1803.10780 [hep-ph].

[40] S. Kumar, R. Sundrum, and Y. Tsai, Non-Gaussian stochastic gravitational waves from phase transitions, *JHEP* **11** (11), 107, arXiv:2102.05665 [astro-ph.CO].

[41] A. Bodas and R. Sundrum, Primordial clocks within stochastic gravitational wave anisotropies, *JCAP* **10** (10), 012, arXiv:2205.04482 [astro-ph.CO].

[42] A. Bodas and R. Sundrum, Large primordial fluctuations in gravitational waves from phase transitions, *Journal of High Energy Physics* **06**, 029 (2023), arXiv:2211.09301 [hep-ph].

[43] V. F. Mukhanov and G. V. Chibisov, Quantum Fluctuations and a Nonsingular Universe, *JETP Lett.* **33**, 532 (1981), [Pisma Zh. Eksp. Teor. Fiz. 33, 549 (1981)].

[44] S. W. Hawking, The Development of Irregularities in a Single Bubble Inflationary Universe, *Phys. Lett.* **115B**, 295 (1982).

[45] A. A. Starobinsky, Dynamics of Phase Transition in the New Inflationary Universe Scenario and Generation of Perturbations, *Phys. Lett.* **117B**, 175 (1982).

[46] A. H. Guth and S. Y. Pi, Fluctuations in the New Inflationary Universe, *Phys. Rev. Lett.* **49**, 1110 (1982).

[47] J. M. Bardeen, P. J. Steinhardt, and M. S. Turner, Spontaneous Creation of Almost Scale - Free Density Perturbations in an Inflationary Universe, *Phys. Rev.* **D28**, 679 (1983).

[48] A. G. Abac *et al.* (LIGO Scientific, VIRGO, KAGRA), Directional Search for Persistent Gravitational Waves: Results from the First Part of LIGO-Virgo-KAGRA's Fourth Observing Run, arXiv 10.48550/arxiv.2510.17487 (2025), arXiv:2510.17487 [gr-qc].

[49] N. Aghanim *et al.* (Planck), Planck 2018 results. VI. Cosmological parameters, *Astron. Astrophys.* **641**, A6 (2020), [Erratum: *Astron. Astrophys.* 652, C4 (2021)], arXiv:1807.06209 [astro-ph.CO].

[50] Y. Akrami *et al.* (Planck), Planck 2018 results. X. Constraints on inflation, *Astron. Astrophys.* **641**, A10 (2020), arXiv:1807.06211 [astro-ph.CO].

[51] N. Bartolo *et al.* (LISA Cosmology Working Group), Probing anisotropies of the Stochastic Gravitational Wave Background with LISA, *JCAP* **11** (11), 009, arXiv:2201.08782 [astro-ph.CO].

[52] Y. Cui, S. Kumar, R. Sundrum, and Y. Tsai, Unraveling cosmological anisotropies within stochastic gravitational wave backgrounds, *JCAP* **10** (10), 064, arXiv:2307.10360 [astro-ph.CO].

[53] K. Schmitz, New Sensitivity Curves for Gravitational-Wave Signals from Cosmological Phase Transitions, *JHEP* **01** (1), 097, arXiv:2002.04615 [hep-ph].

[54] G. Mennasti and M. Peloso, ET sensitivity to the anisotropic Stochastic Gravitational Wave Background, *JCAP* **03** (03), 080, arXiv:2010.00486 [astro-ph.CO].

[55] G. S. F. Guedes, P. P. Avelino, and L. Sousa, Signature of inflation in the stochastic gravitational wave background generated by cosmic string networks, *Phys. Rev. D* **98**, 123505 (2018), arXiv:1809.10802 [astro-ph.CO].

[56] Y. Cui, M. Lewicki, and D. E. Morrissey, Gravitational Wave Bursts as Harbingers of Cosmic Strings Diluted by Inflation, *Phys. Rev. Lett.* **125**, 211302 (2020), arXiv:1912.08832 [hep-ph].

[57] Y. Akrami *et al.* (Planck), Planck 2018 results. IX. Constraints on primordial non-Gaussianity, *Astron. Astrophys.* **641**, A9 (2019), arXiv:1905.05697 [astro-ph.CO].

[58] J. N. Moore and E. P. S. Shellard, On the evolution of Abelian Higgs string networks, arXiv 10.48550/arxiv.hep-ph/9808336 (1998), arXiv:hep-ph/9808336.

[59] K. D. Olum and J. J. Blanco-Pillado, Radiation from cosmic string standing waves, *Phys. Rev. Lett.* **84**, 4288 (2000), arXiv:astro-ph/9910354.

[60] T. Hiramatsu, M. Kawasaki, and K. Saikawa, On the estimation of gravitational wave spectrum from cosmic domain walls, *JCAP* **02** (02), 031, arXiv:1309.5001 [astro-ph.CO].

[61] N. D. Antunes, L. M. A. Bettencourt, and M. Hindmarsh, The Thermodynamics of cosmic string densities in U(1) scalar field theory, *Phys. Rev. Lett.* **80**, 908 (1998), arXiv:hep-ph/9708215.

[62] M. Hindmarsh, S. Stuckey, and N. Bevis, Abelian Higgs Cosmic Strings: Small Scale Structure and Loops, *Phys. Rev. D* **79**, 123504 (2009), arXiv:0812.1929 [hep-th].

[63] P. Auclair, D. A. Steer, and T. Vachaspati, Particle emission and gravitational radiation from cosmic strings: observational constraints, *Phys. Rev. D* **101**, 083511 (2020), arXiv:1911.12066 [hep-ph].

[64] J. M. Quashnock and D. N. Spergel, Gravitational Self-interactions of Cosmic Strings, *Phys. Rev. D* **42**, 2505 (1990).

[65] J. J. Blanco-Pillado and K. D. Olum, Stochastic gravitational wave background from smoothed cosmic string loops, *Phys. Rev. D* **96**, 104046 (2017), arXiv:1709.02693 [astro-ph.CO].

[66] L. Sousa, P. P. Avelino, and G. S. F. Guedes, Full analytical approximation to the stochastic gravitational wave background generated by cosmic string networks, *Phys. Rev. D* **101**, 103508 (2020), arXiv:2002.01079 [astro-ph.CO].

[67] M. Sasaki and E. D. Stewart, A General analytic formula for the spectral index of the density perturbations produced during inflation, *Prog. Theor. Phys.* **95**, 71 (1996), arXiv:astro-ph/9507001.

[68] D. Wands, K. A. Malik, D. H. Lyth, and A. R. Liddle, A New approach to the evolution of cosmological perturbations on large scales, *Phys. Rev. D* **62**, 043527 (2000), arXiv:astro-ph/0003278.

[69] D. H. Lyth, K. A. Malik, and M. Sasaki, A General proof of the conservation of the curvature perturbation, *JCAP* **05** (05), 004, arXiv:astro-ph/0411220 [astro-ph].

[70] A. Afzal *et al.* (NANOGrav), The NANOGrav 15 yr Data Set: Search for Signals from New Physics, *Astrophys. J. Lett.* **951**, L11 (2023), [Erratum: *Astrophys. J. Lett.* 971, L27 (2024), Erratum: *Astrophys. J.* 971, L27 (2024)], arXiv:2306.16219 [astro-ph.HE].

[71] P. Moxhay and K. Yamamoto, Peccei-Quinn Symmetry

Breaking by Radiative Corrections in Supergravity, *Phys. Lett. B* **151**, 363 (1985).

[72] E. Thrane, S. Ballmer, J. D. Romano, S. Mitra, D. Talukder, S. Bose, and V. Mandic, Probing the anisotropies of a stochastic gravitational-wave background using a network of ground-based laser interferometers, *Phys. Rev. D* **80**, 122002 (2009), arXiv:0910.0858 [astro-ph.IM].

[73] E. Thrane and J. D. Romano, Sensitivity curves for searches for gravitational-wave backgrounds, *Phys. Rev. D* **88**, 124032 (2013), arXiv:1310.5300 [astro-ph.IM].

[74] Y. Bao, T. Boybeyi, V. Mandic, and L.-T. Wang, Searching Stochastic Gravitational Wave Background Landscape Across Frequency Bands, arXiv 10.48550/arxiv.2511.19590 (2025), arXiv:2511.19590 [gr-qc].